2014

# Combined QCM-D/GE as a tool to characterize stimuli-responsive swelling of and protein adsorption on polymer brushes grafted onto 3D-nanostructures

Meike Koenig
*Leibniz-Institut für Polymerforschung Dresden*

Tadas Kasputis
*University of Nebraska-Lincoln*, s-tkasput1@unl.edu

Daniel Schmidt
*National University of Singapore*

Keith B. Rodenhausen Jr.
*University of Nebraska-Lincoln*, kbrod@engr.unl.edu

Klaus-Jochen Eichhorn
*Leibniz-Institut für Polymerforschung Dresden*

*See last page for additional authors*

Published in *Analytical and Bioanalytical Chemistry* 406 (2014), pp 7233–7242. doi 10.1007/s00216-014-8154-4
Erratum incorporated from *Analytical and Bioanalytical Chemistry* 407 (2015), pp 1275–1276. doi 10.1007/s00216-014-8343-1

Submitted 23 July 2014; accepted 2 September 2014; published online 21 September 2014
Supplementary material appears following the **References.**



# Combined QCM-D/GE as a tool to characterize stimuli-responsive swelling of and protein adsorption on polymer brushes grafted onto 3D-nanostructures

Meike Koenig,[1,2] Tadas Kasputis,[3,6] Daniel Schmidt,[4,6] Keith B. Rodenhausen,[5,6] Klaus-Jochen Eichhorn,[1] Angela K. Pannier,[3,6,7] Mathias Schubert,[4,6,7] Manfred Stamm,[1,2] and Petra Uhlmann [1,4]

1 Leibniz-Institut für Polymerforschung Dresden e.V., 01069 Dresden, Germany
2 Department of Physical Chemistry of Polymer Materials, Technische Universität Dresden, 01062 Dresden, Germany
3 Department of Biological Systems Engineering, University of Nebraska–Lincoln, Lincoln, NE 68588, USA
4 Department of Electrical Engineering, University of Nebraska–Lincoln, Lincoln, NE 68588, USA
5 Department of Chemical and Biomolecular Engineering, University of Nebraska–Lincoln, Lincoln, NE 68588, USA
6 Center for Nanohybrid Functional Materials, University of Nebraska–Lincoln, Lincoln, NE 68588, USA
7 Nebraska Center for Materials and Nanoscience, University of Nebraska–Lincoln, Lincoln, NE 68588, USA

*Corresponding author* — Petra Uhlmann, email uhlmannp@ipfdd.de

*M. Koenig present address* — Institute of Functional Interfaces, Karlsruhe Institute of Technology, 76344 Eggenstein-Leopoldshafen, Germany
*D. Schmidt present address* — Singapore Synchrotron Light Source, National University of Singapore, Singapore 117603, Singapore

**Abstract**
A combined setup of quartz crystal microbalance and generalized ellipsometry can be used to comprehensively investigate complex functional coatings comprising stimuli-responsive polymer brushes and 3D nanostructures in a dynamic, noninvasive in situ measurement. While the quartz crystal microbalance detects the overall change in areal mass, for instance, during a swelling or adsorption process, the generalized ellipsometry data can be evaluated in terms of a layered model to distinguish between processes occurring within the intercolumnar space or on top of the anisotropic nanocolumns. Silicon films with anisotropic nanocolumnar morphology were prepared by the glancing angle deposition technique and further functionalized by grafting of poly-(acrylic acid) or poly-(*N*-isopropylacrylamide) chains. Investigations of the thermoresponsive swelling of the poly-(*N*-isopropylacrylamide) brush on the Si nanocolumns proved the successful preparation of a stimuli-responsive coating. Furthermore, the potential of these novel coatings in the field of biotechnology was explored by investigation of the adsorption of the model protein bovine serum albumin. Adsorption, retention, and desorption triggered by a change in the pH value is observed using poly-(acrylic acid) functionalized nanostructures, although generalized ellipsometry data revealed that this process occurs only on top of the nanostructures. Poly-(*N*-isopropylacrylamide) is found to render the nanostructures non-fouling properties.

**Keywords:** Thin films, Biomaterials, Interface/surface analysis, Nanostructures, Polymer brushes, Protein adsorption

## Introduction

The formation of functional, responsive coatings, which are able to change their properties upon an external stimulus, for instance, temperature, solvent polarity, pH value, light, or electric current, has been of increasing interest in recent years. To this end, polymeric coatings are ideal candidates[1]. Among the various possible architectures (e.g., block-copolymers, networks, or hydrogels), polymer brushes have proven to be highly suitable [2–4]. Polymer brushes consist of polymer chains tethered by one end to a planar or curved substrate in close proximity to each other such that the chains are forced to stretch away from the surface in a "brush conformation" [5]. These systems are capable of responding to external stimuli, generally by reversible swelling-deswelling behavior. Applying polymer brushes, functional coatings with switchable properties, such as wetting properties [6, 7], adsorption behavior [8–10], ion gating[11], or electrochemical properties [12] have been fabricated. A comprehensive characterization of the responsive behavior and further functionalization is possible using a combined setup of quartz crystal microbalance with dissipation monitoring (QCM-D) together with spectroscopic ellipsometry [13–15].

Another interesting class of coatings are sculptured thin films (STFs), which can be created with variable architectures by glancing angle deposition (GLAD) from a broad variety of different materials [16–20]. Here, electron-beam evaporation at an oblique angle produces nanostructured morphologies, e.g., slanted or straight columns, helices or chevrons, by an atomic shadowing effect. Additionally, the surface of these structures can be modified to add further functionality [21–23]. Recently, we reported on the grafting of poly-(acrylic acid) (PAA) Guiselin brushes onto silicon STFs, which exhibit reversible swelling/deswelling characteristics in response to the pH of the surrounding solution [24].

The combination of responsive polymer brushes with 3D nanostructures constitutes a promising candidate for the engineering of advanced materials for various applications, especially in the field of biotechnology [25, 26]. For instance, the realization of stimulated and controlled uptake and release of biomolecules into and from the free space in between the nanostructures is expected by the use of polymer brushes (Figure 1). In order to develop and apply these novel advanced materials, proper characterization methods are needed to analyze the sample in detail, both directly inside the reaction medium and in a noninvasive manner. These requirements are met by the combined setup of generalized ellipsometry (GE) and QCM-D. In contrast to spectroscopic ellipsometry, GE can be applied to investigate complex, anisotropic samples. Combining the optical method ellipsometry with the acoustical technique QCM-D, it is possible to thoroughly characterize the thickness, composition, and optical and mechanical properties of polymer brush coatings on 3D nanostructures in situ. Particularly, the mechanism of adsorption processes can be tracked, and the stimuli-responsive swelling behavior of the polymer brushes can be observed. While ellipsometry allows the characterization of thickness and composition of the layer via appropriate optical model approaches, QCM-D gives information about thickness, solvent molecules coupled to the polymer brush, and changes in viscoelasticity [27].

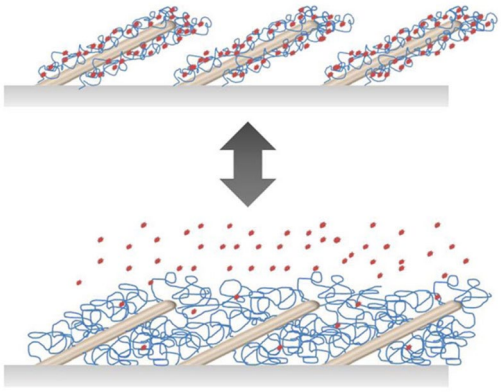

**Figure 1.** Schematic of triggered adsorption and release of biomolecules on stimuli-responsive polymer brushes grafted onto 3D nanostructures.

With this report, we want to promote the establishment of this combined method as a means to characterize complex hybrid materials made from STFs and stimuli-responsive polymer brushes. Thermoresponsive poly-(*N*-isopropylacrylamide) (PNIPAAm) brushes were grafted to silicon STFs and the responsive properties were investigated. Secondly, as a demonstration of the performance of these materials in the field of biotechnology, the adsorption of the model protein bovine serum albumin (BSA) on PNIPAAm and PAA brushes on nanostructured films was studied using the combined setup of GE and QCM-D (Figure 2).

## Experimental

### Characterization methods

*Generalized ellipsometry* Ellipsometry is a non-destructive method to characterize thin films by measuring the change in optical polarization of a beam of light, which is reflected from a surface [28–30]. For complex samples (for instance, optically anisotropic), generalized ellipsometry is used. To describe the measured change in polarization upon reflection from the sample, the Mueller-Stokes formalism is applied, which can describe polarized, partially polarized, and unpolarized light. The 4 × 4 Mueller matrix characterizes the light-sample interaction and relates the state of polarization of the incident beam with

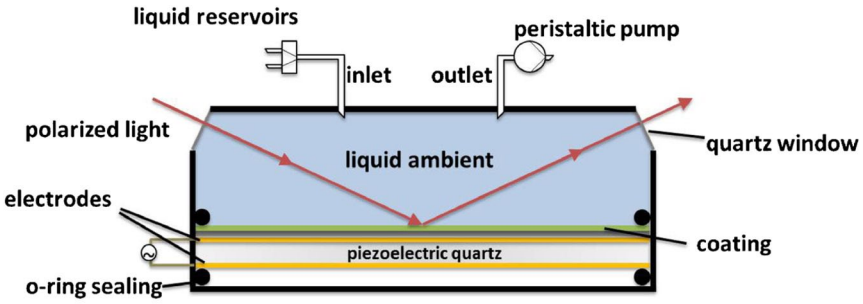


**Figure 2.** Schematic of the combined setup of QCM-D and GE.

the state of polarization of the reflected beam, which are both described by a Stokes vector:

$$S' = \hat{M} S \tag{1}$$

(where $S$ is the Stokes vector describing the incident beam, $S'$ is the Stokes vector describing the reflected beam, and $\hat{M}$ is the Mueller matrix). Similar to previously published STF ellipsometric procedures [23, 31, 32], spectroscopic Mueller matrix data obtained by GE were analyzed with WVASE32 software (Version 3.768b, J.A. Woollam Co., Inc.). Best-match model calculations were performed using an anisotropic Bruggeman effective medium approximation (AB-EMA) approach, which allows for the determination of geometrical STF parameters as well as fractions of multiple constituents. The optical model (Figure 3) includes the underlying substrate (gold-coated quartz sensor) and a biaxial AB-EMA layer, which consists of a Si/$SiO_2$ constituent ($f_{STF}$), an ambient fraction ($f_{Ambient}$; either air or buffer solution), and an organic constituent (polymer or biomolecule, $f_{Organic}$), where the wavelength-dependent refractive index is described by a Cauchy dispersion lineshape:

$$n(\lambda) = \frac{A + B}{\lambda^2} \tag{2}$$

using $A = 1.5$ and $B = 0.01$, under the condition that the extinction coefficient $k$ equals zero. The material of the Si/$SiO_2$ constituent is described by an isotropic Bruggeman-EMA, consisting of 20 vol% $SiO_2$ to accommodate for a native oxide layer of approximately 2 to 3 nm, and silicon. Si optical constants were determined by a multisample analysis of bare Si STF using a single Tauc-Lorentz oscillator. Finally, the model comprises a layer above the AB-EMA layer to account for possible organic material on top of the slanted columns, described by a Cauchy dispersion lineshape ($A = 1.5$, $B = 0.01$, $k = 0$).

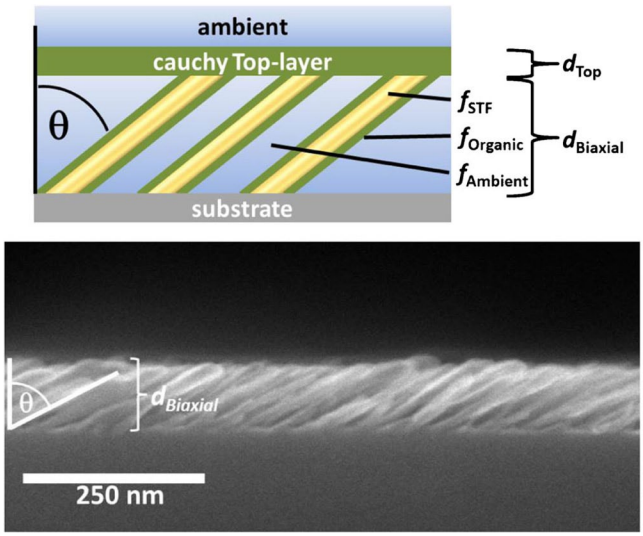


**Figure 3.** Schematic of the optical model of STF functionalized with polymer brushes used for the evaluation of GE data (*upper part*); SEM images of a STF before functionalization with polymer brushes (*lower part*, Adapted with permission from Kasputis et al. [24]; copyright 2013 American Chemical Society).

*QCM-D* The measuring principle of the QCM is based on the inverse piezoelectric effect, where the application of alternating voltage to a piezoelectric crystal leads to an oscillatory motion [33–36]. The resonance frequency of the quartz sensor is sensitive to changes induced by the contact with the ambient and processes occurring on its surface, for instance, adsorption processes, which can be observed in situ with high temporal resolution. Since the QCM is sensitive to both the properties of the thin film and the bulk medium, reference measurements of the bare sensor in the same medium are necessary to separate the two components. QCM-D is a special mode of operation, developed by Rodahl et al. [37]. In this "ring-down" mode, the applied alternating voltage is turned off intermittently, leaving the oscillations to decay. The time of decay is related to the loss of energy (dissipation $D_n$), for instance, due to contact of the surface of the quartz with a viscous medium or a thin viscoelastic film.

QCM-D data were analyzed either using the Sauerbrey equation or the Voigt-Voinova approach. For homogeneous rigid films, showing only small shifts in dissipation ($\Delta D_n/n - \Delta F_n/n << 4 \times 10^{-7}$ $Hz^{-1}$, for a sensor with the fundamental resonance

frequency $F_F$ = 5 MHz), the Sauerbrey equation is valid. Here, the areal mass of the film will include the mass of the adsorbate plus the mass of the solvent inside the adsorbate layer and additional solvent, which is acoustically coupled to the quartz surface, that is, moving with the oscillatory motion of the quartz sensor. If $\Delta D_n$ is sufficiently large, the QCM-D is sensitive to the viscoelastic properties of the film, described by the complex shear modulus. By a continuum model based on the analysis of shear wave propagation in viscous media, the response of the QCM can be related to the areal mass density of the film, bound to the surface of the sensor under no-slip conditions, and its viscoelastic properties [38–40].

Shifts in frequency and dissipation of the odd overtones $j$ = 5, 7, 9, 11 with reference to the measurement with the smallest dissipation value, were analyzed using either a Voigt-Voinova model for one homogeneous viscoelastic layer with a fixed density of 1 g $cm^{-3}$ or the Sauerbrey relation using the software QTools (Q-Sense, Frölunda, Sweden). As a reference for analyzation of data recorded at varying temperatures, a bare sample was measured with the same temperature changes. The measured temperature-dependent change in frequency and dissipation was subtracted from the raw data of measurements of sensors functionalized with polymer brushes.

## Preparation of STF

STFs were fabricated by electron-beam evaporation of Si onto gold-coated quartz crystal microbalance sensors (QSense Inc., Linthicum Heights, MD) for further analysis. Si pellets (Super Conductor Materials, Inc., Tallman, NY) were evaporated at a vapor flux angle of 88° with respect to the substrate normal, to fabricate slanted columns. The background pressure of the evaporation chamber was in the low $10^{-8}$ mbar range. Samples were deposited at a constant vapor flux of approximately 3.5 Å $s^{-1}$, which was measured with a deposition controller mounted normal to the flux direction.

## Brush preparation on STF

Polymer brushes were prepared similarly to the grafting-to method established for flat substrates [41]. Following STF deposition, samples were cleaned with absolute ethanol (Pharmco, USA) and dried with $N_2$ gas. For cleaning and activation, samples were placed into an oxygen plasma chamber (SPI Plasma Prep II plasma cleaner; Structure Probe, Inc., West Chester, PA, USA) for 1 min at 100 W. A macromolecular anchoring layer was spin-coated onto the samples from a 0.02 wt% solution of poly(glycidyl methacrylate) (PGMA, $M_n$ = 17,500 g $mol^{-1}$, $M_w/M_n$ = 1.12; Polymer Source, Inc., Canada) in methyl-ethyl ketone (MEK, Sigma-Aldrich, USA) and annealed in vacuum for 10 min at 110 °C. On this anchoring layer, the polymer brush layer was grafted in the next step. For PAA Guiselin brushes, a 1 wt% solution of PAA ($M_n$ = 26,500 g/mol, $M_w/M_n$ = 1.7; Polymer Source, Inc., Canada), dissolved in absolute ethanol, was spin-coated onto the samples and annealed in vacuum for 30 min at 80 °C. For PNIPAAm brushes, a 1 wt% solution of carboxy-terminated PNIPAAm ($M_n$ = 56,000 g $mol^{-1}$; Polymer Source, Inc., Canada), dissolved in chloroform ($CHCl_3$, Sigma-Aldrich, USA), was spin-coated onto the samples and annealed in vacuum for 16 h at 170 °C. Excess polymer was extracted by stirring the samples in absolute ethanol for 30 min at room temperature.

## Instrumentation

*Generalized ellipsometry rotation scans* GE measurements of the samples in dry state were taken before and after every step of polymer brush grafting onto STF using a M-2000V spectroscopic ellipsometer (J.A. Woollam Co., Inc., Lincoln, NE, USA) equipped with a rotation stage to acquire 11 out of the 16 Mueller matrix elements at multiple discrete wavelengths between 400 and 1,700 nm, at four angles of incidence (AOI: 45°, 55°, 65°, and 75°), and 0–360° rotation (in steps of 12°) in the polar azimuth plane.

*Combined in situ generalized ellipsometry and quartz crystal microbalance with dissipation* For in situ characterization, a combined QCM-D/GE setup consisting of an E1 QCM-D and an ellipsometry-compatible module (Q-Sense, Inc.), mounted onto the sample stage of an M-2000 spectroscopic ellipsometer (J.A. Woollam Co., Inc., NE, USA) with a fixed AOI of 65°, capable of measuring 11 out of the 16 Mueller matrix elements, was used. The ellipsometry-compatible module is an airtight liquid flow chamber, into which the sample is inserted for in situ analysis; the module has windows for the probing light beam of an ellipsometry measurement (Figure 2). Flow of liquid medium is ensured by means of Tygon polyurethane tubing (U.S. Plastics Corp., Lima, OH), which is connected to a peristaltic flow pump (Ismatec IPC high precision multichannel dispenser, IDEX Health & Science GmbH, Wertheim-Mondfeld, Germany).

For temperature-dependent measurements in between 20 and 38°C, the ellipsometry-compatible module temperature was controlled by the QCM-D software, and the system temperature was changed step-wise in 30-min intervals. Temperature experiments were performed under static conditions.

BSA adsorption experiments were performed in 0.01 M sodium phosphate (Sigma-Aldrich, USA) buffer solution at 20 °C under flowing conditions (1 ml $min^{-1}$). The sample was first rinsed in pH 5 buffer solution, then a solution of 0.25 mg $ml^{-1}$ bovine serum albumin (BSA, A6003, defatted; Sigma-Aldrich, USA) in pH 5 buffer was introduced. Desorption was performed in rinsing steps with pH 5, pH 7.4, and again pH 5 buffer solution.

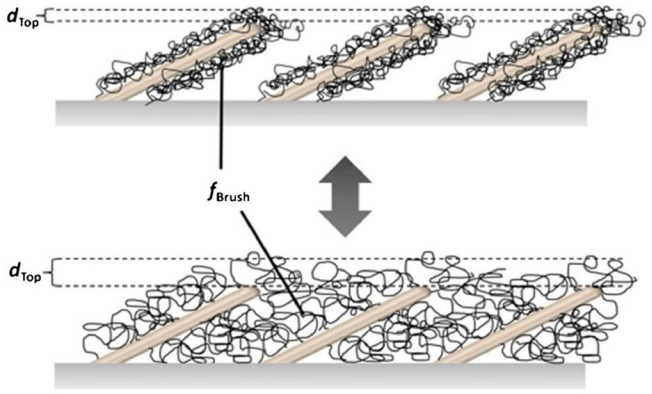


**Figure 4.** Schematic of hypothesized brush deswelling and swelling within STFs.

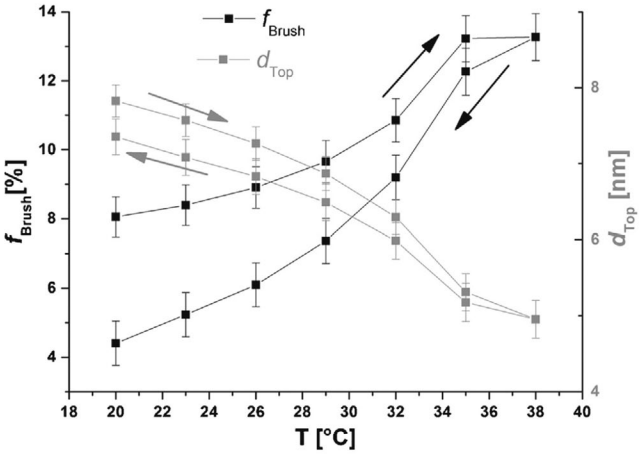


**Figure 5.** Results of the best-match model calculation of GE measurements of temperature induced swelling and deswelling of PNIPAAm brushes on STFs.

In addition to experiments with brush-coated STF, a reference in situ characterization of each STF sample was performed in the bare state before the grafting of polymer brushes. For comparison, also one protein adsorption experiment was performed on a bare, uncoated STF sample (see supporting information).

## Results and discussion

Polymer brushes were grafted to STF similar to the already established method of grafting polymer brushes to flat surfaces [41], and as already reported for the preparation of PAA brushes on STFs [24]. GE rotation scans were conducted in dry state after each step of the preparation. Since during these experiments the sample is measured under four different angles of incidence and 30 different in-plane orientations, the obtained data is more sensitive to small variations of the structured surface, such as volume fractions or slanting angle, than the data obtained during the subsequent in situ measurements. Thus, it is possible to characterize the sample comprehensively, as a reference for changes occurring during the in situ experiments. The best-match model parameters for the GE rotation scans of the PNIPAAm brushes were a brush volume fraction of $f_{Brush}$ ~ 28 % and a top-layer thickness of $d_{Top}$ ~ 3 nm after extraction of excess polymer. Using the average size of a single column, as measured from SEM images ($r$ ~10 nm (Figure 2, [24])), and the structural parameters from the best-match GE model, the thickness of the brush layer on the columns can be calculated via the total surface area of the structured sample and the grafted amount of polymer. Thus, a total surface area of 2.5 μm$^2$ of the nanostructures per 1-μm$^2$ sample area was estimated. Together with a PNIPAAm amount of 11.5 mg m$^{-2}$, this corresponds to a hypothesized homogeneous PNIPAAm layer with a thickness of 4 nm in dry state and a grafting density of 0.05 nm$^{-2}$ [5] (using the bulk density $\rho_{PNIPAAm}$ = 1.097 g cm$^{-3}$ [42]).

### Responsive swelling of polymer brushes on STFs

In situ GE and QCM-D measurements were conducted simultaneously, investigating stimuli-induced polymer brush swelling/deswelling on STFs (Figure 4). The pH-responsive swelling of PAA brushes grafted onto STFs had been reported in an earlier work [24].

*Thermoresponsive swelling of PNIPAAm on STFs* Figure 5 depicts results of the best-match model calculation of GE measurements of PNIPAAm brushes on STFs in DI water for one temperature cycle between 20 and 38 °C, where the error bars represent the 90 % confidence intervals determined by the best-match model calculation. Measurements were conducted at static conditions. Only measurements taken after no further variation of QCM-D data upon reaching the next temperature step was recorded were taken into account. Data of the first in situ measurement at 20 °C were analyzed under variation of all model parameters. Further changes in the optical response upon a change in temperature can be described by changes in $f_{Brush}$ and $d_{Top}$ only. PNIPAAm is a temperature-responsive polymer with a phase transition temperature at $T_c$ ~32 °C in pure water [43]. As the temperature increases the polymer gradually deswells, which is detected by an increase in $f_{Brush}$ and a decrease in $d_{Top}$. Because the thickness of the top-layer is best-match model calculated using typical values of a dry organic layer for the refractive index, an effective dry thickness is obtained and not the thickness of the polymer layer swollen with solvent. An increase of the thickness upon swelling of the polymer chains would result in an according decrease of the refractive index due to dilution of the optical density of the polymer layer. Best-match model calculation of the actual swollen thickness by simultaneous variation of the refractive index was not

possible, since the recorded data did not carry enough sensitivity to distinguish between the strongly correlated parameters $d_{Top}$ and $n_{Top}$. The obtained value of $d_{Top}$ is thus a measure of the amount of dry polymer on top of the nanostructures $A_{Top}$, which can be calculated by

$$A_{Top} = d_{Top}\rho_{Polymer} \quad (3)$$

if the density of the dry polymer layer $\rho_{Polymer}$ is known.

Compared to measurements on planar samples, the phase transition of PNIPAAm brushes on the structured samples is less sharp, probably due to the lower grafting density on the columns [44, 45]. Upon decreasing the temperature again, the reversed behavior can be seen and the polymer chains collapse back into the intercolumnar space.

In Figure 6, results of the best-match model calculation of QCM-D data analyzed with a Voigt-Voinova approach for viscoelastic layers are shown. Upon deswelling of the PNIPAAm chains, solvent molecules are expelled from the acoustically coupled layer and the film becomes more rigid resulting in a decrease in areal mass and viscosity. Upon re-cooling of the sample, a slight hysteresis is detected, due to inter- and intra-chain hydrogen bonds [46–48]. Compared to PNIPAAm brush swelling on planar samples [45], the phase transition is less pronounced and the signal change is much less, due to the lower grafting density on the nanostructures. Nevertheless, these experiments show that PNIPAAm brushes can be prepared on STFs with temperature-responsive properties, and detailed investigation on the anisotropic sample is feasible using QCM/GE.

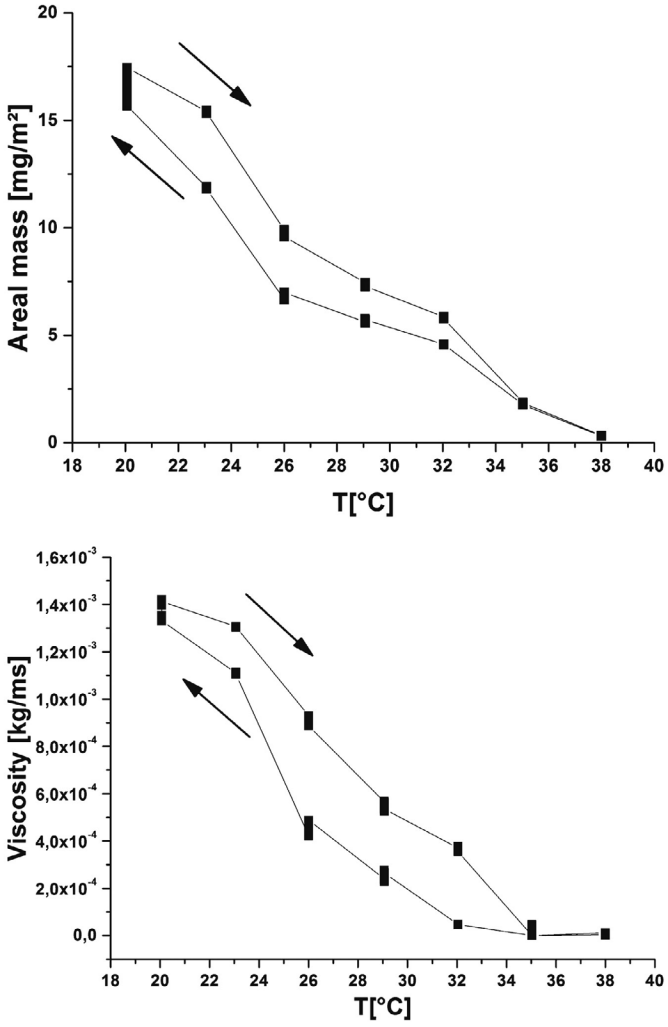


**Figure 6.** Best-match model parameters of QCM-D measurements of temperature-induced swelling and deswelling of PNIPAAm brushes on STFs. *Top*, change in areal mass; *bottom*, change in viscosity.

## Protein adsorption on brushes on STFs

As a proof-of-concept study for future biological or sensor applications, the adsorption of the model protein BSA to polymer brushes prepared on STFs was studied.

When a material comes into contact with biological fluids, for instance, in sensor systems or on implants, the adsorption of proteins is the first step of several cascadic processes. Therefore, the understanding, and even more the control, of this process is regarded as a key factor in the development of biomaterials [49–51]. The interaction between protein and surface is governed by various forces as hydrophobic or van derWaals interactions. Regarding the adsorption of proteins on charged and hydrophilic surfaces, electrostatic interactions are considered to be of the highest influence on the adsorption process. Albumins are commonly used model proteins due to their importance in the blood plasma and their ready availability due to a relatively easy isolation and purification procedure. They appear in an ellipsoidal shape with a major axis of 14 nm and a minor axis of 4 nm [52].

Experiments were performed in 0.01-M sodium phosphate buffer solution. The course of experiments was as follows: (I) swelling of the polymer in pH 5 buffer solution, (II) adsorption of BSA (0.25 mg $ml^{-1}$ in pH 5 buffer), (III) rinse with pH 5 buffer solution, (IV) rinse with pH 7.4 buffer solution, and (V) rinse with pH 5 buffer solution. Combined QCM-D and GE measurements were conducted to monitor the process in situ.

*Protein adsorption to PAA brushes on STFs* On flat samples, BSA has been shown to adsorb on PAA Guiselin brushes both under electrostatic attractive and moderately repulsive conditions [14]. In this study, adsorption under electrostatic attractive conditions at pH 5 was investigated, since a higher driving force for the proteins to diffuse into the polymer layer inside the intercolumnar space is to be expected.

Figure 7 depicts results of best-match model calculations of GE measurements taken during the adsorption process of BSA to PAA brushes on STFs. The changes in GE data can be described by changes in the volume fraction of an organic component $f_{Organic}$ and the top-layer thickness $d_{Top}$. The parameter for the top layer is calculated using typical values for the description of the refractive index of a dry organic material, thus ignoring the swelling of the polymer and the protein. Changes in $d_{Top}$ are a measure of a change in the amount of organic material on top of the nanostructures. Upon introduction of BSA to the measurement cell (II), a fast and pronounced increase of $d_{Top}$ from 5 to 22 nm is suggested by the best-match model calculations, while $f_{Organic}$ first increases slightly from 33 to 36% followed by a slow decrease. Almost all proteins are adsorbed in the polymer layer on top of the STF, with only a small percentage of adsorption to the polymer inside the intercolumnar space. A reason could be a sterical hindrance presented by the swollen polymer layer blocking the space in between the columns (distance between individual columns ~20 nm (Figure 2, [24])). Additionally, the STFs used for these specific experiments exhibited a high slanting angle of ~75–80°, which had increased by ~15° from the initial ~60–65° during in situ experiments of the bare STF sample, performed before grafting of the polymer layer. STFs with lower initial slanting angle and larger intercolumnar space are expected to show a higher uptake of proteins into the intercolumnar space.

Upon changing of the solution to pH 5 buffer solution without protein again (III), almost no change in $f_{Organic}$ and $d_{Top}$ is detected, proving the high retention capabilities of the PAA-STF-system. By changing the pH of the buffer solution to pH 7.4 (IV), an abrupt decrease both in $f_{Organic}$ and $d_{Top}$ can be seen. In this step, the pH value is increased above the isoelectric point (IEP) of the protein (pH($IEP_{BSA}$)=5.6 [53]), resulting in an overall negative charge. At the same time, more carboxylic groups along the PAA chains get deprotonated, causing a high electrostatic repulsion and thereby releasing the protein from the polymer brush. Due to the higher swelling degree of the PAA chains, $d_{Top}$ is larger and $f_{Organic}$ smaller compared to the original value at pH 5 before BSA adsorption. A final rinse with pH 5 buffer solution (V) causes PAA to deswell again, which is detected as an increase in $f_{Organic}$ and a decrease in $d_{Top}$. Since the original values are not restored, a small amount of remaining BSA molecules is suggested to remain in the polymer coating. This had been also observed in experiments on flat surfaces [14].

The corresponding change in areal mass, derived from QCM-D data, is shown in Figure 8. Since the change in dissipation is small compared to the change in frequency, a Sauerbrey approach can be used to describe the detected frequency change. With the introduction of BSA (II), a fast increase in areal mass up to ~38 mg/m$^2$ is observed, decreasing only slightly during the rinsing with pure pH 5 buffer solution (III). Upon rinsing with pH 7.4 buffer solution (IV), at first an increase in areal mass is detected, due to the deprotonation and swelling of PAA chains. This is rapidly followed by a fast decrease in areal mass, caused by desorption of BSA molecules under now strongly repulsive electrostatic conditions. At this point of the experiment, the Sauerbrey approach has to be regarded with caution, since the change in frequency and therefore also the change in areal mass, becomes overtone-dependent, due to the more viscoelastic properties of the film. After rinsing with pH 5 buffer solution (V), the frequency becomes overtone-independent again, and the areal mass decreases to ~4 mg/m$^2$. A

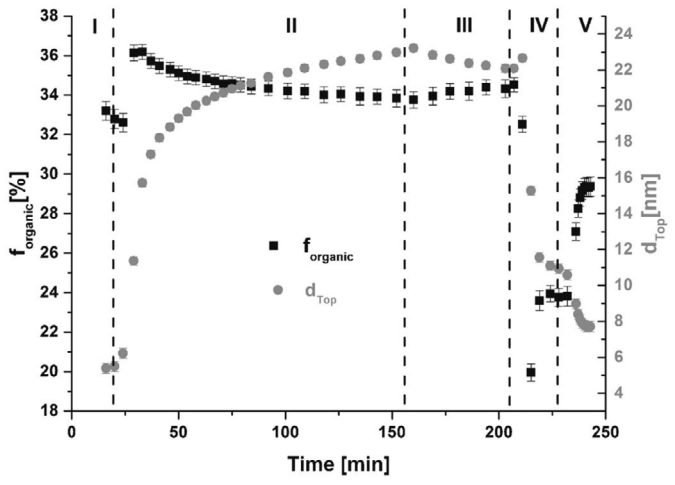


**Figure 7.** Best-match model parameters of GE measurements of the adsorption of BSA on PAA brushes on STF, (*I*) p

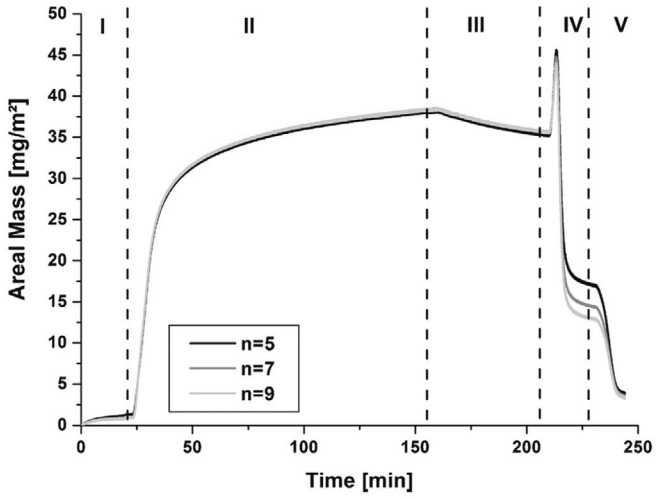


**Figure 8.** Change in areal mass, derived from QCM-D measurements of the adsorption of BSA on PAA brushes on STF, (*I*) pH 5, (*II*) BSA adsorption, (*III*) pH 5, (*IV*) pH 7.4, and (*V*) pH 5

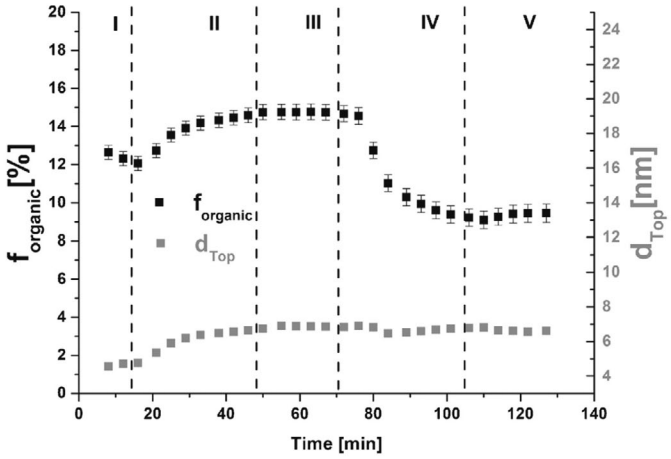


**Figure 9.** Best-match model parameters of GE measurements of the adsorption of BSA on PNIPAAm brushes on STF, (*I*) pH 5, (*II*) BSA adsorption, (*III*) pH 5, (*IV*) pH 7.4, and (*V*) pH 5.

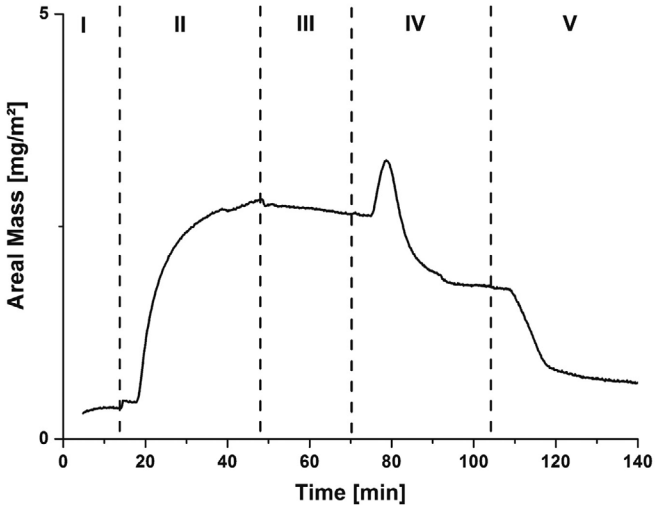


**Figure 10.** Change in areal mass, derived from QCM-D measurements of the adsorption of BSA on PNIPAAm brushes on STF, (*I*) pH 5, (*II*) BSA adsorption, (*III*) pH 5, (*IV*) pH 7.4, and (*V*) pH 5.

small amount of BSA remains in the polymer brush and cannot be washed off by raising the pH. Compared to experiments with BSA adsorption on planar samples, about the same adsorbed amount of BSA at pH 5 is observed on the STF [14]. This strongly supports the findings of the analysis of GE data that adsorption of protein only takes place in the top-layer above the STF and not in the intercolumnar space. Due to this similarity with experiments on planar samples, no further quantitative studies were pursued.

*Protein adsorption to PNIPAAm on STFs* PNIPAAm brushes on planar samples had been found to be resistant to protein adsorption [54]. Therefore, the aim was to create non-fouling structured coatings by grafting PNIPAAm chains to Si-STFs. Figure 9 depicts the results of the best-match model calculations of GE measurements taken during the adsorption process of BSA to PNIPAAm brushes on STFs. As proposed, the change in GE data upon BSA adsorption is much less than compared to the adsorption to PAA brushes on STFs. Upon introduction of BSA (II), $d_{Top}$ increases only by 2.5 nm, whereas the change in $f_{Organic}$ of ~3 % is about the same as observed with PAA brushes on STFs. This indicates that while the uptake of BSA into the intercolumnar space is about the same as for PAA, only a very small amount of BSA is adsorbing in the top layer. As the pH value of the buffer solution is increased to pH 7.4 (IV), BSA is expected to desorb from the surface, because of the increased electrical repulsion between the now overall negatively charged proteins. Interestingly, the results of the best-match model calculations suggests that while $d_{Top}$ stays almost constant, only $f_{Organic}$ decreases by ~6 %. This would imply that while BSA is desorbing from the polymer coating, at the same time, re-arrangement of the polymer layer occurs, with an increasing proportion of PNIPAAm chains swelling out of the intercolumnar space.

In QCM-D measurements, the detected change both in frequency and dissipation is small; therefore, the Sauerbrey approach was used to determine the change in areal mass (Figure 10). During the rinsing with a solution of BSA in pH 5 buffer (II), only ~2.3 mg/m$^2$ of BSA is adsorbed to the sample. This value is even lower than observed during the adsorption of BSA to bare Si-STFs out of a more diluted solution of 0.01 mg ml$^{-1}$ BSA in pH 5 buffer (see supporting information). Upon rinsing with a solution of higher pH (IV), the areal mass initially increases, probably caused by the incorporation of counter ions to the more negatively charged proteins. Thereafter, proteins desorb and the areal mass decreases to ~1.5 mg/m$^2$. The second decrease in areal mass, upon rinsing with pH 5 buffer solution (V), can be explained by the loss of counter ions of proteins that remain on the sample surface. Overall, QCM-D and GE results are in agreement, and both investigation techniques suggest that almost no protein adsorption takes place on PNIPAAm brushes grafted to Si-STFs.

Thus, PAA and PNIPAAm brushes can be used to control the adsorption of proteins on nanostructures. This is of crucial importance for applications, for instance, in biosensor systems, where unspecific adsorption has to be avoided.

## Summary

Novel functional coatings were created by preparation of stimuli-responsive PAA and PNIPAAm brushes on Si-STFs with nanocolumnar morphology. The combined method of QCM-D and GE was found to be a suitable characterization tool

for noninvasive, dynamic in situ investigations of the swelling characteristics of the polymer brushes, as well as the process of protein adsorption to these complex coatings. While QCM-D detects overall change of areal mass and viscoelasticity on the surface, interpretation of GE data with a layered model can be used to distinguish between processes occurring within the intercolumnar space or on top of the anisotropic columnar layer. Changes in the areal mass, viscoelasticity and the optical response with varying temperature proved the grafting of PNIPAAm chains to the STFs in a temperature-responsive manner. For future biological and sensor applications, the adsorption of the model protein BSA to PAA and PNIPAAm brushes was investigated. The QCM-D/GE study of the adsorption process found that BSA adsorbs to PAA brushes on STFs under attractive electrostatic conditions. However, the analysis of the GE data suggests that only adsorption in the top layer above the STF and the change in areal mass detected by QCM-D is similar to experiments with PAA on flat samples. Nevertheless, pH-responsive uptake, retention, and release of the model protein were achieved. Both QCM-D and GE data demonstrate that PNIPAAm brushes can be used to render Si-STFs non-fouling properties.

In future studies, QCM-D/GE investigations will be used to assist in the optimization of the developed hybrid nanostructured coatings, by variation of the architecture of the sculptured thin films or the combined grafting of several types of stimuli-responsive polymers. Thus, stimuli-responsive immobilization and manipulation of biomolecules could be achieved. Since the applied grafting-to technique can be employed to graft various types of functionalized polymers, the coating of the nanostructures can be tailored to the respective application.

**Acknowledgments** —The authors acknowledge the financial support by the German Science Foundation (DFG) and the U.S. National Science Foundation (NSF) within the DFG-NSF "Materials World Network" under award numbers STA 324/49-1 and EI 317/6-1, and by NSF under award numbers EPS-1004094, CBET-1254415, and CMMI-1337856.

## References

1. Cohen Stuart MA, Huck WT, Genzer J, Müller M, Christopher O, Stamm M, Sukhorukov G, Szleifer I, Tsukruk VV, Urban M, Winnik F, Zauscher S, Luzinov I, Minko S (2010) Nat Mater 9:101
2. Azzaroni O (2012) J Polym Sci 50:3225
3. Ayres N (2010) Polym Chem 1:769
4. Chen T, Ferris R, Zhang J, Ducker R, Zauscher S (2010) Prog Polym Sci 35:94
5. Brittain WJ, Minko S (2007) J Polym Sci Part A: Polym Chem 45:3505
6. Stratakis E, Mateescu A, Barberoglou M, Vamvakaki M, Fotakis C, Anastasiadis SH (2010) Chem Commun 46:4136
7. Liu X, Ye Q, Yu B, Liang Y, Liu W, Zhou F (2010) Langmuir 26:12377
8. Ionov L, Stamm M, Diez S (2006) Nano Lett 6:1982
9. Mi L, Bernards MT, Cheng G, Yu Q, Jiang S (2010) Biomaterials 31:2919
10. Kumar S, Tong X, Dory YL, Lepage M, Zhao Y (2013) Chem Comm 49:90
11. Yameen B, Ali M, Neumann R, Ensinger W, Knoll W, Azzaroni O (2009) J Am Chem Soc 131:2070
12. Tam TK, Pita M, Motornov M, Tokarev I, Minko S, Katz E (2010) Adv Mater 22:1863
13. Domack A, Prucker O, Rühe J, Johannsmann D (1997) Phys Rev E 56:680
14. Bittrich E, Rodenhausen K, Eichhorn KJ, Hofmann T, Schubert M, Stamm M, Uhlmann P (2010) Biointerphases 5:159
15. Koenig M, Rodenhausen KB, Schmidt D, Eichhorn KJ, Schubert M, Stamm M, Uhlmann P (2013) Part Syst Charact 30:931
16. Robbie K, Brett MJ (1997) J Vac Sci Technol A 15:1460
17. Seto MW, Dick B, Brett MJ (2001) J Micromech Microeng 11:582
18. Zhao YP, Ye DX, Wang GC, Luc TM (2003) Nanotubes and nanowires. SPIE, Bellingham
19. Lakhtakia A, Messier R (2005) Sculptured thin films: Nanoengineered morphology and optics. SPIE, Bellingham
20. Hawkeye MM, Brett MJ (2007) J Vac Sci Technol A 25:1317
21. Tsoi S, Fok E, Sit JC, Veinot JGC (2006) Chem Mater 18:5260
22. Albrecht O, Zierold R, Patzig C, Bachmann J, Sturm C, Rheinländer B, Grundmann M, Görlitz D, Rauschenbach B, Nielsch K (2010) Phys Status Solidi B 247:1365
23. Schmidt D, Schubert E, Schubert M, Appl Phys Lett (2012) 100:011912
24. Kasputis T, Koenig M, Schmidt D, Sekora D, Rodenhausen KB, Eichhorn KJ, Uhlmann P, Schubert E, Pannier AK, Schubert M, Stamm M (2013) J Phys Chem C 117:13971
25. Liu H, Liu X, Meng J, Zhang P, Yang G, Su B, Sun K, Chen L, Han D, Wang S, Jiang L (2013) Adv Mater 25:922
26. de Groot GW, Demarche S, Santonicola MG, Tiefenauer L, Vancso GJ (2014) Nanoscale 6:2228
27. Rodenhausen KB, Schubert M (2011) Thin Solid Films 519:2772
28. Schubert M (1996) Phys Rev B 53:4265
29. Tompkins HG, Irene EA (2005) Handbook of ellipsometry. William Andrew Publishing, Norwich
30. Fujiwara H (2007) Spectroscopic ellipsometry—Principles and applications. Wiley, Chichester
31. Rodenhausen KB, Schmidt D, Kasputis T, Pannier AK, Schubert E, Schubert M (2012) Opt Express 20:5419
32. Schmidt D, Schubert M (2013) vol 114, p 083510
33. Sauerbrey G (1959) Z Phys 155:206
34. Kanazawa KK, Gordon JG (1985) Anal Chem 57:1770

35. Schuhmacher R (1999) Chem Unserer Zeit 5:268
36. Reviakine I, Johannsmann D, Richter R (2011) Anal Chem 83:8838
37. Rodahl M, Höök F, Krozer A, Brzezinski P, Kasemo B (1995) Rev Sci Instrum 66:3924
38. Voinova M, Jonson M, Kasemo B (1997) J Phys: Condens Matter 9:7799
39. Voinova M, Rodahl M, Jonson M, Kasemo B (1999) Physica Scripta 59:391
40. Voinova M, Jonson M, Kasemo B (2002) Biosens Bioelectron 17:835
41. Swaminatha Iyer K, Zdyrko B, Malz H, Pionteck J, Luzinov I Macromolecules 36:6519
42. Bae YH, Okano T, Kim SW (1990) J Polym Sci Pol Phys 28:923
43. Schild HG, Tirrell DA (1990) J Phys Chem 94:4352
44. Yim H, Kent S, Mendez S, Lopez GP, Satija S, Seo Y (2006) Macromolecules 39:3420
45. Bittrich E, Burkert S, Müller M, Eichhorn KJ, Stamm M (2012) P. Uhlmann, Langmuir 28:3439
46. Wang X, Qiu X, Wu C (1998) Macromolecules 31:2972
47. Cheng H, Shen L, Wu C (2006) Macromolecules 39:2325
48. Lu Y, Zhou K, Ding Y, Zhang G, Wu C (2010) Phys Chem Chem Phys 12:3188
49. Norde W (2008) Biointerfaces Colloids and Surfaces B 61:1
50. Vroman L (2009) Materials 2:1547
51. Fenoglio I, Fubini B, Ghibaudi EM, Turci F (2011) Adv Drug Deliver Rev 63:1186
52. Squire P, Moser P, O'Konski C (1968) Biochemistry 7:4261
53. Soetewey F, Rosseneu-Motreff M, Lamote R, Peeters H (1972) J Biochem 71:705
54. Burkert S, Bittrich E, Kuntzsch M, Müller M, Eichhorn KJ, Bellmann C, Uhlmann P, Stamm M (2010) Langmuir 3:1786

## 0.1 Best-match model calculation results for GE rotation scans

GE rotation scans in dry state were measured after the fabrication of the STF sample, after an *in situ* measurement of the uncoated STF in buffer solution, after the polymer brush preparation and after an *in situ* measurement of the polymer-coated STF in buffer solution. Results are shown in Table 1 and Table 2. The error values represent the 90% confidence intervals calculated by the best-match model calculation.

Table 1: Best-match model calculation parameters for the preparation of PAA on STF

| | post fabrication | post bare insitu | post PAA brush | post brush insitu |
|---|---|---|---|---|
| $d_{\mathrm{Biaxial}}$[nm] | 79±0.1 | 42±0.1 | 38±0.1 | 37±0.1 |
| $\theta$[°] | 64.5±0.02 | 79.1±0.03 | 81.9±0.05 | 81.2±0.04 |
| $f_{\mathrm{STF}}$[%] | 16.6±0.05 | 23.2±0.05 | 26.4±0.06 | 23.9±0.02 |
| $f_{\mathrm{Organic}}$[%] | 0±0.2 | 0±0.2 | 18±0.3 | 19±0.1 |
| $d_{\mathrm{Top}}$[nm] | 0±0.1 | 0±0.1 | 3±0.1 | 0±0.1 |

Table 2: Best-match model calculation parameters for the preparation of PNIPAAm on STF

| | post fabrication | post bare insitu | post PAA brush | post brush insitu |
|---|---|---|---|---|
| $d_{\mathrm{Biaxial}}$[nm] | - | 45±0.1 | 37±0.1 | 35.7±0.1 |
| $\theta$[°] | - | 78.1±0.4 | 82.6±0.04 | 82±0.1 |
| $f_{\mathrm{STF}}$[%] | - | 26.2±0.06 | 20.8±0.03 | 20.5±0.04 |
| $f_{\mathrm{Organic}}$[%] | - | 0±0.3 | 28.1±0.2 | 32.3±0.3 |
| $d_{\mathrm{Top}}$[nm] | - | 0±0.1 | 3±0.1 | 0±0.1 |

## 0.2 Protein Adsorption on bare STF

For comparison protein adsorption was performed on a bare, uncoated STF sample in 0.01 M sodium phosphate (Sigma Aldrich, USA) buffer solution at 20 °C under flowing conditions ($1\,\mathrm{ml\,min^{-1}}$). The sample was first rinsed in pH 5 buffer solution, then a solution of $0.01\,\mathrm{mg\,ml^{-1}}$ bovine serum albumin (BSA, A6003, defatted, Sigma Aldrich, USA) in pH 5 buffer was introduced. Desorption was performed in rinsing steps with pH 5 and pH 7.4 buffer solution. Figure 1 displays the change in areal mass derived from QCM-D measurement using the Sauerbrey equation.

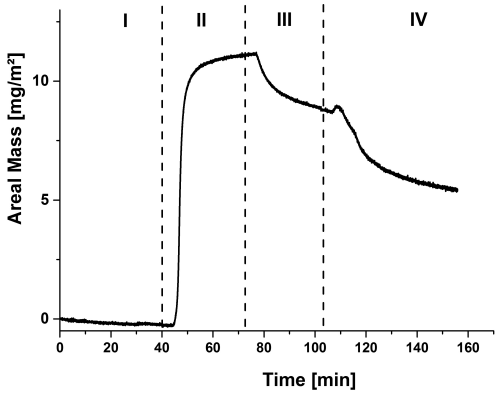


Figure 1: Change in areal mass, derived from QCM-D measurements of the adsorption of BSA on bare STF, (I) pH 5, (II) BSA adsorption, (III) pH 5, (IV) pH 7.4